OPEN

Horseradish Peroxidase Inactivation: Heme Destruction and Influence of Polyethylene Glycol

Liang Mao[1], Siqiang Luo[1], Qingguo Huang[2] & Junhe Lu[3]

[1]State Key Laboratory of Pollution Control and Resource Reuse, School of the Environment, Nanjing University, Nanjing 210023, P. R. China, [2]College of Agricultural and Environmental Sciences, Department of Crop and Soil Sciences, University of Georgia, Griffin, GA 30223, USA, [3]Department of Environmental Science and Engineering, Nanjing Agricultural University, Nanjing, 210093, P. R. China.

Horseradish peroxidase (HRP) mediates efficient conversion of many phenolic contaminants and thus has potential applications for pollution control. Such potentially important applications suffer however from the fact that the enzyme becomes quickly inactivated during phenol oxidation and polymerization. The work here provides the first experimental data of heme consumption and iron releases to support the hypothesis that HRP is inactivated by heme destruction. Product of heme destruction is identified using liquid chromatography with mass spectrometry. The heme macrocycle destruction involving deprivation of the heme iron and oxidation of the 4-vinyl group in heme occurs as a result of the reaction. We also demonstrated that heme consumption and iron releases resulting from HRP destruction are largely reduced in the presence of polyethylene glycol (PEG), providing the first evidence to indicate that heme destruction is effectively suppressed by co-dissolved PEG. These findings advance a better understanding of the mechanisms of HRP inactivation.

Horseradish peroxidase (HRP) is a classic heme enzyme having widespread use in pollution control, biomedical research, and organic synthesis. HRP catalyzes one-electron oxidation of phenolic and other aromatic substrates to form radicals via a Chance-George mechanism[1–3]. Free radicals generated from phenolic substrates in aqueous phase react with each other to form oligomers, and soluble coupling products serve as enzyme substrates in further oxidative coupling reactions until larger polymers that precipitate from solution are formed[4,5]. Because polymerized products formed from such coupling reactions can readily settle from water and/or become immobilized in soil/sediment systems, enzyme-enhanced oxidative coupling reactions have potential applications for water treatment[6–8] and soil remediation[9–12]. Such potentially important applications suffer however from the fact that the enzyme becomes quickly inactivated during phenol oxidation and polymerization.

Three pathways have been identified for HRP inactivation: 1) reaction with H_2O_2 (i.e. active enzyme intermediate compounds react with excess peroxide to form different inactive species)[13,14]; 2) sorption/occlusion by polymeric products (i.e. HRP adsorbs on precipitated coupling products and its active sites become occluded)[15]; and 3) Heme destruction (i.e. strong reagents generated during the enzymatic reaction, such as free radicals, react with and inactivate the heme center in HRP)[16,17]. Relative contributions of the three inactivation pathways vary with reaction conditions. The first pathway is largely suppressed in the presence of reductive donor substrates (e.g. phenols) because they compete with H_2O_2 for the active enzyme intermediates[18,19]. The second pathway is not evident unless large quantities (grams per liter) of precipitated polymeric products are formed[20]. The third pathway appears to predominate at reaction conditions commonly encountered in environmental applications[21]. Unfortunately, mechanisms associated with HRP inactivation by heme destruction are not yet fully understood on the molecular level, although we have demonstrated that this pathway involves the release of iron atoms from HRP[20].

It has been found that HRP inactivation is significantly mitigated when certain dissolved polymers, such as polyethylene glycol (PEG), are present in the reaction solution, which leads to effective enhancement of enzyme turnover capacity. PEG has thus been proposed as an additive in HRP-based water treatment operations to enhance process efficiency[15,22,23]. In HRP-mediated phenol reaction systems, HRP has been found to be retained effectively in aqueous phase when PEG is present, but to co-precipitate with the polymeric products in the absence

of PEG[15]. This observation reveals that enzyme sorption/occlusion by polymeric products (the second inactivation pathway mentioned above) is mitigated by PEG. Whether PEG impacts other HRP inactivation pathways, particularly the heme destruction pathway remains unknown.

In the study reported here we performed a series of carefully designed experiments to demonstrate that iron releases resulting from HRP inactivation during HRP-mediated phenol reactions are largely reduced in the presence of PEG. This observation provides the first evidence to indicate that HRP inactivation via heme destruction is effectively suppressed by co-dissolved PEG. We extracted and analyzed the heme center from aqueous HRP using liquid chromatography with mass spectrometry (LC-MS) to study the mechanism of HRP inactivation by heme destruction. These findings provide information for optimizing engineering applications that involve HRP reactions, and advance an understanding of the mechanisms of HRP inactivation. The information is also useful for studies concerning the inactivation behaviors of other heme-containing enzymes.

Results

Phenol conversion and precipitated product formation. Results for phenol conversion and precipitated product formation are displayed in Figure 1. As shown in the figure, nearly complete conversion of phenol was achieved at all reaction conditions tested, and considerable amount of products was precipitated. Obviously, more precipitate was formed as more phenol/H_2O_2 concentration was employed. Slightly more phenol remained and somewhat less precipitate was formed in the reaction systems without PEG than those with 2% PEG. This apparently results from the mitigation effects of PEG on HRP inactivation as shown in Figure 2.

H_2O_2 consumption. As described in Methods, residual H_2O_2 after reactions were tested using peroxide test strips. The tests showed negative for all reaction conditions tested. HRP catalyzes the one-electron oxidation of phenolic substrates to form radicals via a Chance-George mechanism. The phenoxyl radicals generated react with each other to form oligomers, while the soluble coupling products can still serve as phenolic substrates and undergo further oxidative coupling until larger polymers that precipitate from solution are formed[4]. The apparent stoichiometric ratio between phenol and peroxide thus shifts from the theoretical value of 2 : 1
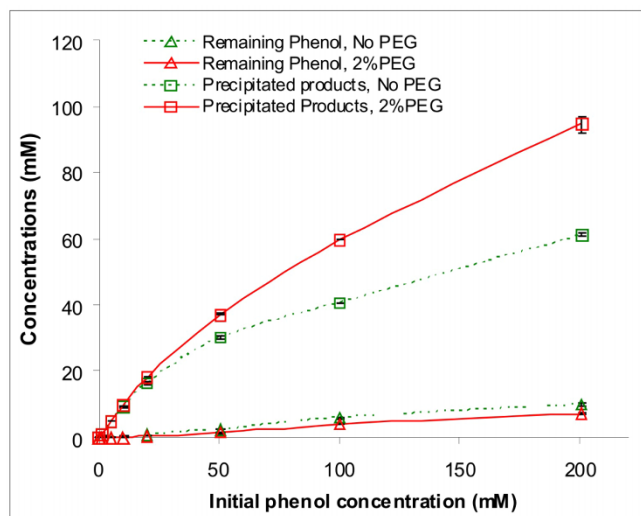
Figure 1 | Phenol conversion and precipitate formation at different reaction conditions. The initial H_2O_2 concentration is half of the initial phenol concentrations as shown in the abscissa. Reaction time is 60 min. Error bars indicate the standard deviation of triplicate samples.
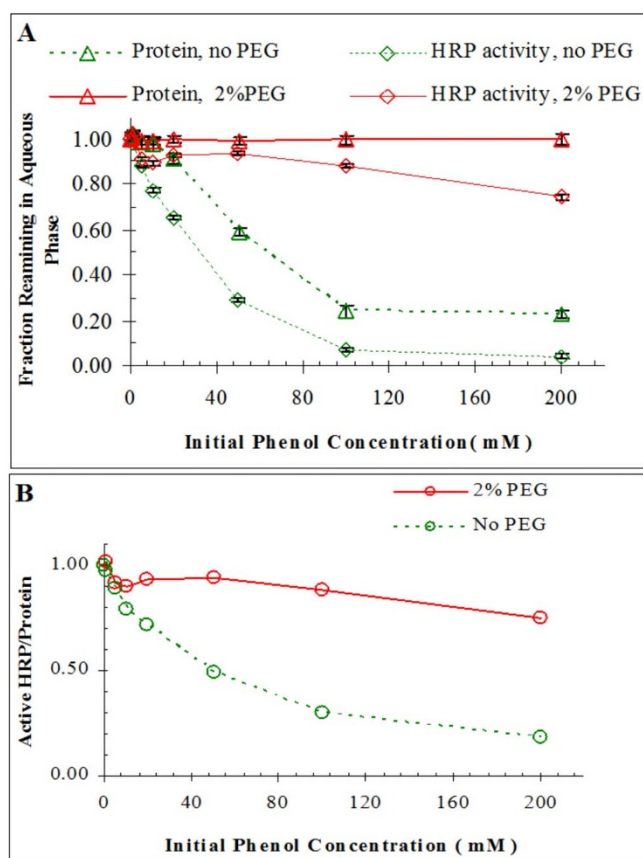
Figure 2 | (A) Fractions of total protein and HRP activity remaining in the supernatant as a function of phenol/H_2O_2 concentrations; **(B)** the ratio between active HRP and protein content in the aqueous phase. Initial HRP concentration is 0.1 mM. Initial H_2O_2 concentration is half of the initial phenol concentrations as shown in the abscissa. Reaction time is 60 min. Error bars indicate the standard deviation of triplicate samples.

reflecting a catalytic cycle, and approaches a value of 1 : 1 as the polymeric coupling products grow in size if they do so strictly by the radical coupling mechanism[24]. A 2 : 1 ratio between phenol and H_2O_2 was used in this study to ensure a complete consumption of H_2O_2 during the reaction, which was confirmed by the H_2O_2 strip tests. This limited HRP inactivation by reactions with excess H_2O_2 in solutions (The first pathway mentioned in Introduction). In our earlier report[20], we have demonstrated that if H_2O_2 was consumed during the reaction, the contribution of H_2O_2-based HRP inactivation is very little.

The fact that H_2O_2 was completely consumed indicates that the reactions measured in this study are all limited by H_2O_2, which explains the relatively minor difference in the outcome of the reactions for systems with and without PEG as shown in Figure 1. The protection effects of the PEG on HRP are reflected in Figure 2 that higher HRP activity was preserved after reactions.

Total protein and HRP activity. Figure 2A displays the fractions of total protein and HRP activity remaining in the supernatant after reactions at varying initial phenol/H_2O_2 concentrations. As shown in Figure 2A, the protein in systems without PEG present was increasingly removed from the solution phase as more precipitates were formed; while in the presence of PEG protein remained almost completely in solution across different reaction conditions. This confirms that PEG can effectively retain HRP in aqueous phase. Also shown in Figure 2A, the remaining fractions of HRP activity in both the sample without PEG and that with PEG are smaller than those of the protein content. This indicates that a fraction of the

dissolved HRP was inactivated, suggesting that a pathway other than precipitate entrapment plays a role inactivating HRP. Since H_2O_2 was completely consumed under all reaction conditions, the contribution of H_2O_2-based HRP inactivation is not significant. It is therefore likely that HRP inactivation by heme destruction (the third inactivation pathway) leads to the discrepancy in the remaining fractions of HRP activity and protein content. Figure 2B displays ratios of the remaining active HRP and protein content for samples with and without PEG present. The much larger ratios for the samples with PEG clearly indicate that the inactivation pathway, whatever it may be, is largely suppressed in the presence of PEG.

Iron release. Figure 3 presents iron concentrations detected in the filtrates of solutions that had undergone reactions at various phenol/H_2O_2 concentrations. A membrane with 3 kDa molecular weight cutoff was used, and neither protein nor HRP activity was detected in any of the filtrates. It is thus certain that the iron in the filtrate is released from HRP molecules as a result of heme destruction. The much lower iron concentrations in the solutions with PEG provide direct evidence that HRP inactivation by heme destruction is largely suppressed by the presence of PEG. Standard addition tests indicate that recovery of iron cations by the membrane filtration is near 90% for the product solution without PEG and near 80% for that with PEG. This precludes the potential alternative interpretation that the differences in filtrate iron concentrations shown in Figure 3 can be caused by solution effects on filtration.

Another interesting observation to be made with respect to Figure 3 is that the detected free iron concentrations account for only a fraction of the total HRP inactivated beyond precipitate entrapment. For example, as shown in Figure 2A, in the solution with 200 mM phenol and 2% PEG about 26% HRP (26 μM) was inactivated with no protein loss to the precipitate, but iron release at this condition is only 3.4 μM as shown in Figure 3. Figure 2B shows that for the solution with 200 mM phenol and without PEG, 19% of the dissolved protein remained active. Assuming that the same active HRP/protein ratio holds for the protein entrapped in the precipitate, it can be estimated that 81 μM of HRP was inactivated by pathways other than entrapment in this product solution. However, only 24 μM free iron was detected in the same solution as shown in Figure 3. It can thus be postulated that there are inactive HRP species in the solutions other than those with iron released, suggesting that heme destruction may occur in a successive manner.
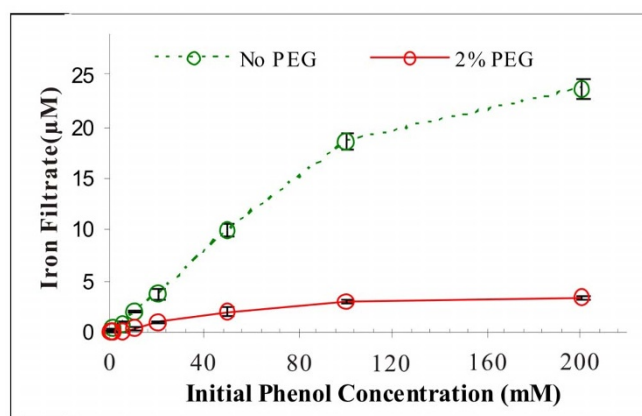
Heme destruction. Heme is a prosthetic group that consists of an iron atom in the center of a large heterocyclic organic ring called a porphyrin and the heme in HRP is the catalytic reaction center[25–28]. To explore possible heme destruction during HRP inactivation, heme was extracted from aqueous HRP in selected samples and quantified. As shown in Figure 4A, the UV-vis spectra of the extractants from the reaction sample and the control without addition of H_2O_2 is different. Figure 4B shows relative concentrations of heme detected in the solution that had undergone reactions at various phenol/H_2O_2 concentrations. As shown in this figure, the concentration of heme in reactions without PEG was lower than those with PEG. Comparing Figures 4B and 2A, it is evident that the remaining fractions of heme are close to those of remaining HRP activity and smaller than those of remaining protein. This suggests that HRP inactivation is accompanied with heme transformation and some of the remaining proteins either do not contain heme or contain a heme that has been transformed. Heme extraction was further analyzed with LC-MS to explore the possible heme transformation products. As shown in Figure 5A, native heme has a retention time of 12.5 min and generates a molecular ion of m/z
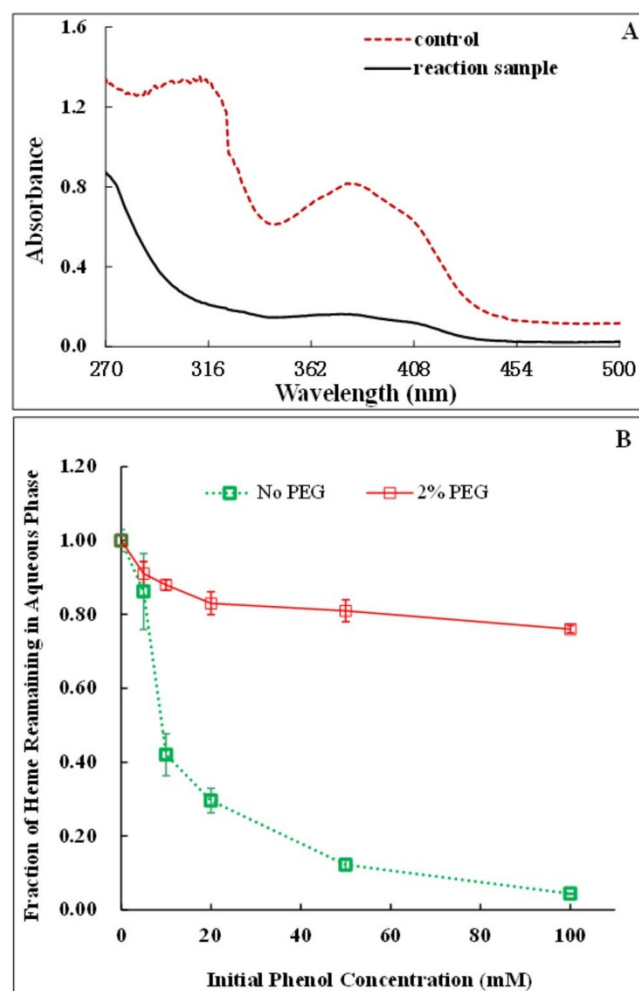

Figure 4 | (A) UV spectrum of the heme extraction extracted from the regular HRP (control) and the incubated HRP (reaction sample); (B) Fractions of heme remaining in aqueous phase after reactions at various phenol/H_2O_2 concentrations. Experimental condition: (A) Initial HRP, phenol and H_2O_2 concentration is 0.1 mM, 100 mM and 50 mM, respectively; (B) Initial HRP concentration is 0.1 mM. Initial H_2O_2 concentration is half of the initial phenol concentrations as shown in the abscissa. Reaction time is 60 min. Error bars indicate the standard deviation of triplicate samples.

Figure 3 | Iron concentrations detected in solutions after reactions at various phenol/H_2O_2 concentrations and membrane filtration. Initial HRP concentration is 0.1 mM. Initial H_2O_2 concentration is half of the initial phenol concentrations as shown in the abscissa. Reaction time is 60 min. Error bars indicate the standard deviation of triplicate samples.

616.2 (see Figure 5B), which was consistent with the *m/z* value reported in earlier studies[29–31]. The concentration of heme decreased in reaction system with 100 mM phenol and 50 mM H_2O_2. A new peak appeared for the reaction sample but not for the control samples at the retention time of 8 min (peak 1 in Fig. 5A) which is presumed to be the product of heme upon destructive reaction. Its MS is shown in Figure 5C, with *m/z* 607.3 as the possible molecular ion.

Earlier studies have proved that heme in HRP could undergo reactions with different substrates at the vinyl groups[31,32] or the *meso*

carbons[16,17,29,33,34] (see Fig. 6A). Wojciechowski and Ortiz de Montellano[35] further confirmed that selection of the reaction site depended on the molecular bond dissociation energies for RH (substrate) → R· (substrate radical) + H· at 298 K. High-energy (≥90 ± 1 kcal/mol) radicals add to the *meso* carbon and less energetic radicals (<90 ± 1 kcal/mol) add to heme vinyl groups. The data obtained using resonance Raman and FTIR measurements in our earlier study suggests that a significant amount of phenoxyl radical exist in solution and probably also in the heme pocket[20]. The molecular bond dissociation energies for phenol → phenolic radical + H· at
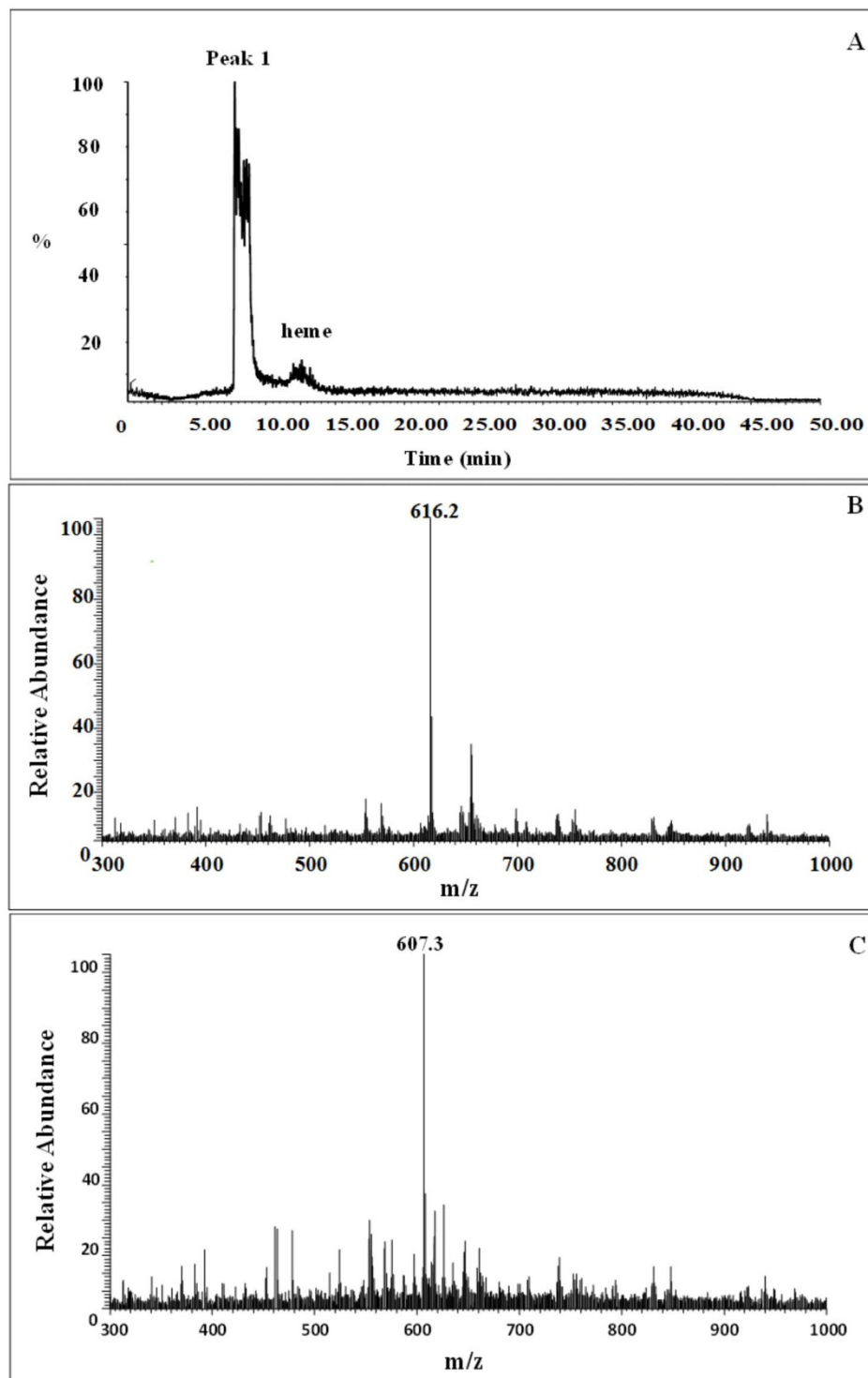
Figure 5 | (A) LC chromatography of the heme and the possible product (peak 1) extracted from reaction sample; (B) LC-MS analysis of the heme; and (C) LC-MS analysis of the possible reaction product (peak 1 in Figure 5A). Initial HRP, H_2O_2 and phenol concentration is 0.1 mM, 50 mM and 100 mM.
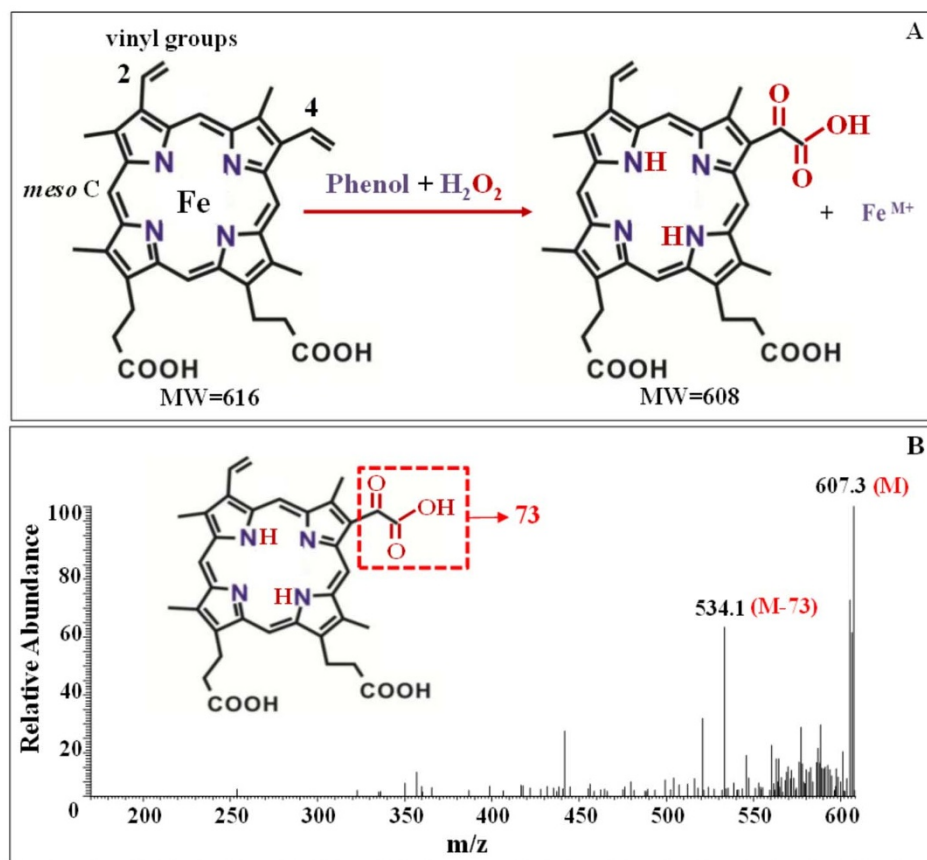
Figure 6 | (A) Proposed mechanism for heme destruction in HRP-mediated phenol reaction; (B) Secondary MS spectrometry of possible product resulting from LC-MS analysis and its possible structures.

298 K is 88 kcal/mol[36]. As such, we propose that the phenolic radical attacks regioselectively to either 2- or 4-vinyl group (see Fig. 6A). The masses of the product follow a pattern of (MW-56 (iron) +16 (oxygen) × 3, where MW is 616). This leads us to speculate that the product was formed via the heme transformation which occurred at the vinyl group accompanied by the addition of oxygen and iron release (see Fig. 6A). As shown in Fig. 6A, the oxidation may occur at the 4-vinyl group not at the 2-vinyl group position because it is the only exposed edge of the heme in HRP[32,34]. Secondary MS spectrometry of the product was attempted for further molecular characterization and the results were presented in Figure 6B. The m/z 607.3 (M) was chosen as the MS/MS precursor ion. As shown in Fig. 6B, an intense fragment ion at m/z 534.1 was yielded from the precursor ion. It indicated the loss of the group of (-C_2O_3H, MW = 73) which was corresponding to the oxidized 4-vinyl group (see Fig. 6B). Our proposal of product identification was further supported by the results of secondary MS spectrometry.

Discussion

As already noted, previous studies on substrate-mediated HRP inactivation which includes three pathways indicate that heme destruction may predominate at reaction conditions commonly encountered in environmental applications. The direct evidence to support the heme destruction in HRP caused by radical attack, however, is not found. The present findings clearly show that the heme destruction is accompanied by iron releases and prosthetic group change. The prosthetic group change are supported by (a) UV-vis spectrum changes (Fig. 4A), (b) decrease of heme contained in HRP (Fig. 4B), and (c) analysis of the data obtained using LC-MS. Analysis of the possible product found when the prosthetic group is extracted

from HRP after turnover of phenol establishes that the product was generated by oxidative attack of phenoxyl radical on the heme vinyl group and release of iron. These findings advance the better understanding of the mechanisms of HRP inactivation and the information is useful for HRP re-design to protect HRP from inactivation and enhance HRP reactivity towards compounds of specific interest[37].

HRP-mediated coupling process provides a novel strategy to control certain emerging trace-level contaminants in water treatment practice. Opposite to degradation, it mimics the humification process and incorporates small molecules of contaminants into polymers with larger molecular sizes and therefore leads to detoxification or removal[38–40]. It has been found that the presence of PEG in the reaction solution significantly mitigated the HRP inactivation when large quantities (grams per liter) of precipitated polymeric products are formed. Researchers concluded that this mitigation was attributed to the protection of HRP from sorption by polymeric products[15]. However, PEG still mitigated the HRP inactivation in environmental applications where the substrate concentration was low and no significant quantities of precipitated polymeric products were formed. The molecular understanding of this phenomenon was not clear. In this study, we clearly demonstrated that the predominant inactivation pathway at the reaction conditions encountered in environmental applications was HRP destruction. Heme consumption and iron releases resulting from HRP destruction are largely reduced in the presence of PEG, providing the first evidence to indicate that heme destruction is effectively suppressed by co-dissolved PEG. This information is useful for optimizing engineering applications that involve HRP reactions to control trace-level contamination.

Methods

Materials. Horseradish peroxidase (Type I, RZ = 1.3), hydrogen peroxide (30.8%), phenol (99+%), 2,2′-azino-bis(3-ethylbenz-thiazoline-6-sulfonic acid) (ABTS) (98%, in diammonium salt form), glacial acetic acid and phenol-UL-14C (51.4 mCi mmol^{-1}) were obtained from Sigma Chemical Co. (St. Louis, MO). FeCl$_3$·6H$_2$O (98%) was purchased from Aldrich (Milwaukee, WI). PEG (3350, 50%) from Hampton Research (Aliso Viejo, Ca.), ScintiSafe Plus 50% liquid scintillation cocktail from Fisher Scientific (Fairlawn, NJ), Coomassie® protein assay reagent kit from Pierce Biotechnology (Rockford, IL) and Quantofix® peroxide test strips from Macherey-Nagel, (Germany).

Reaction setup. Air-tight 5 mL borosilicate centrifuge vials fitted with Teflon coated caps were used as reactors. Reactions were carried out in a 10 mM phosphate buffer, with the initial HRP concentration fixed at 100 μM. Initial phenol concentrations ranging from zero to 200 mM, and initial H$_2$O$_2$ concentrations were half of that of phenol. The constant 2 : 1 ratio between initial phenol and H$_2$O$_2$ concentrations was selected to ensure complete consumption of peroxide during the reaction. The same reaction conditions were also tested for solutions with 2% (m/m) PEG included. The reactors were agitated at 150 rpm for one hour after the reaction had been initiated by addition of peroxide to reactors as the last reagent. After the one-hour reaction period the reactor vial was centrifuged at 1620 g for 10 min, and the supernatant transferred to another centrifuge tube and centrifuged again at 10,000 g for 10-min to ensure complete separation of the solid products. Samples were then taken from the supernatant for analyses of protein content, HRP activity, heme concentration and residual H$_2$O$_2$. The remaining supernatant was then transferred to a centrifugal ultrafiltration device (Pall Life Science, Ann Arbor, MI) and centrifuged at 8,000 g for 60 min with temperature maintained at 20°C to pass the solution through the membrane. The membrane employed was low protein binding bio-inert type, having a nominal molecular weight cutoff at 3 kDa. Samples from the filtrates were taken for analyses of protein content and HRP activity again and iron concentration.

Separate experiments employing ^{14}C-labeled phenol at the exactly same series of conditions described above were also carried out for the determination of phenol conversion and precipitate product formation. After reaction and double centrifugation to separate resulting solid products from solution phase, supernatant samples were taken to measure residual phenol concentration and ^{14}C radioactivity.

All experiments described above were carried out in triplicate and results were reported as the average with standard deviation.

Standard addition tests. Standard addition tests were performed to examine the recovery of dissolved iron by membrane filtration. These tests were carried out using the same procedure described earlier in solutions with 100 μM HRP, 200 mM phenol, and 100 mM H$_2$O$_2$, and with and without PEG, respectively. After reaction and double centrifugation, two 2 mL samples were withdrawn from the supernatant. 19.5 μM FeCl$_3$·6H$_2$O was added to one of the sample, and nothing to the other. All samples was transferred to centrifugal ultrafiltration devices, and centrifuged to pass solutions through the membrane. Iron concentrations were detected in each filtrate, and recovery of the added iron was calculated. Triplicate tests were conducted and the average (±SD) of the recovery ratios were 88.3 (±3.0)% and 79.7 (±1.4)% for samples with and without PEG, respectively.

A control test was also conducted using the same reagent combination as above, but only for a solution without PEG. After reaction and double centrifugation, two 2 mL aliquots were withdrawn from the supernatant. 2% PEG was added to one of the sample, and nothing to the other. Both samples were then filtered and detected for iron as described above. Recovery ratio for the sample with 2% PEG addition was calculated as iron concentration in this sample divided by that in the sample without PEG addition. The average (±SD) of triplicate tests was 99.7 (±1.0)%.

Chemical analyses. The Coomassie® (Pierce Biotechnology, Rockford, IL) protein assay was used to determine total protein concentration remaining in aqueous phase[41] and ABTS as substrate to measure HRP activity[42]. One unit of HRP activity is defined as that amount catalyzing the oxidation of 1 μmol of ABTS per minute. The total dissolved iron was measured using ICP-OES (Optima 2000 DV, Perkin-Elmer). Residual hydrogen peroxide was tested using Quantofix® peroxide test strips (Macherey-Nagel, Germany). The detection limit of the test strips is 15 μM as specified by the supplier. Residual phenol concentration was analyzed using an Agilent 1100 HPLC system equipped with a Phenomenex C18 column (250 × 2.0 mm, 5 μm particle size). The mobile phase was maintained at 0.4 mL min^{-1}, comprising acetonitrile and DI water (35 : 65), both containing 1% acetic acid. Phenol concentration was determined by florescence detector at 275 nm excitation and 312 nm emission wavelengths, and phenol conversion was calculated by mass balances. Residual ^{14}C radioactivity was measured using a Beckman LS6500 liquid scintillation counter (LSC) (Beckman Instruments, Inc.), reflecting the concentration of dissolved ^{14}C species including phenol and dissolved phenol-coupling products. Quantities of precipitated products were thus calculated by mass balance and expressed as phenol equivalent concentration.

Isolation and identification of heme. HRP-catalyzed phenol oxidation in solutions without PEG was examined to study possible changes occurring to heme during the reaction. The reaction was carried out using the same procedure described above in solutions with 100 μM HRP, 100 mM phenol and 50 mM H$_2$O$_2$. Reactors that had phenol or H$_2$O$_2$ absent served as blank controls. After reaction and double centrifugation, three 0.5 mL samples were withdrawn from the supernatant. A

literature method was then used to extract and analyze heme[16,17]. Each sample was added in sequence, 1 mL DI water, 0.4 mL glacial acetic acid, and 200 mg NaCl. The sample was then mixed with 2 mL ethyl acetate, and centrifuged (2500 rpm, 10 min) to separate the aqueous and organic layers. The organic layers were withdrawn, pooled, washed with H$_2$O, and then analyzed using HPLC and LC-MS and UV/Vis spectrometry.

HPLC analysis was performed on a C18 column (250 × 2.0 mm, 5 μm particle size) eluted with 7 : 3 : 1 methanol/H$_2$O/acetic acid at a flow rate of 1 mL min^{-1}, and heme was monitored by its characteristic absorbance at 400 nm with a diode array detector. LC-MS analysis was conducted on a Thermo LCQ Advantages instrument (Quest LCQ Duo, USA) with electrospray ionization. The LC separation was achieved using a Beta Basic-C18 HPLC column (150-mm × 2.1 mm, 5 μm Thermo, USA) with a mobile phase of water (with 0.02% acetic acid)/acetonitrile (1 : 1) at a flow rate of 0.2 mL min^{-1}. The mass spectrometer was set at 3.5 kV capillary voltage, 25 V cone voltage, 350°C desolvation temperature and 120°C source temperature. The further identification of possible product was also analyzed by LC-MS/MS. The system operated in selected reaction monitoring mode. The molecular ions obtained from full scan mode were chosen as the precursor ions.

The UV/Vis spectra of the extraction solution were scanned using 752-UV/Vis spectrophotometer (ShangHai Spectrum instruments, Co., LTD.) and the scanned wavelength was ranged from 270 to 500 nm with the interval 1 nm. Ethyl acetate was prepared as control.

1. Chance, B. The properties of the enzyme-substrate compounds of HRP and peroxides. *Arch. Biochem. Biophys.* **22**, 224–252 (1949).
2. George, P. The chemical nature of the 2nd-hydrogen peroxide compound formed by cytochrome C-peroxidase and horseradish peroxidase. 2. Formation and decomposition. *Biochem. J.* **54**, 220–230 (1953).
3. George, P. The chemical nature of the 2nd-hydrogen peroxide compound formed by cytochrome C-peroxidase and horseradish peroxidase. 1. Titration with reducing agents. *Biochem. J.* **54**, 267–276 (1953).
4. Yu, J., Taylor, K. E., Zou, H., Biswas, N. & Bewtra, J. K. Phenol conversion and dimeric intermediates in horseradish peroxidase-catalyzed phenol removal from water. *Environ. Sci. Technol.* **28**, 2154–2160 (1994).
5. Junker, K., Zandomeneghi, G., Guo, Z., Kissner, R., Ishikawa, T., Kohlbrechere, T. & Walde, P. Mechanistic aspects of the horseradish peroxidase-catalysed polymerisation of aniline in the presence of AOT vesicles as templates. *RSC Adv.* **2**, 6478–6495 (2012).
6. Auriol, M., Filali-Meknassi, Y., Tyagi, R. D. & Adams, C. D. Oxidation of natural and synthetic hormones by the horseradish peroxidase enzyme in wastewater. *Chemosphere* **68**, 1830–1837 (2007).
7. Klibanov, A. M., Tu, T. & Scott, K. P. Peroxidase-catalyzed removal of phenols from coal-conversion waste waters. *Science* **221**, 259–261 (1983).
8. Weber, W. J. Jr. & Huang, Q. Inclusion of persistent organic pollutants in humification processes: direct chemical incorporation of phenanthrene via oxidative coupling. *Environ. Sci. Technol.* **37**, 4221–4227 (2003).
9. Bollag, J. M. Decontaminating soil with enzymes. *Environ. Sci. Technol.* **26**, 1876–1881 (1992).
10. Dec, J. & Bollag, J. M. Phenoloxidase-mediated interactions of phenols and anilines with humic materials. *J. Environ. Qual.* **29**, 665–676 (2000).
11. Huang, Q. & Weber, W. J. Jr. Peroxidase-catalyzed coupling of phenol in the presence of model inorganic and Organic Solid Phases. *Environ. Sci. Technol.* **38**, 5238–5245 (2004).
12. Bhandari, A. & Xu, F. Impact of peroxidase addition on the sorption-desorption behavior of phenolic contaminants in surfaces soils. *Environ. Sci. Technol.* **35**, 3163–3168 (2001).
13. Nakajima, R. & Yamazaki, I. The mechanism of oxyperoxidase formation from freely peroxidase and hydrogen-peroxide. *J. Biol. Chem.* **262**, 2576–2581 (1987).
14. Arnao, M. B., Acosta, M., Del Rio, J. A., Varon, R. & Garcia-Canovas, F. A kinetic study on the suicide inactivation of peroxidase by hydrogen peroxide. *Biochim. Biophys. Acta.* **1041**, 43–47 (1990).
15. Nakamoto, S. & Machida, N. Phenol removal from aqueous-solutions by peroxidase-catalyzed reaction using additives. *Water Res.* **26**, 49–54 (1992).
16. Ator, M. A. & Ortiz de Montellano, P. R. Protein control of prosthetic heme reactivity: reaction of substrates with the heme edge of horseradish peroxidase. *J. Biol. Chem.* **262**, 1542–1551 (1987).
17. Ator, M. A., David, S. K. & Ortiz de Montellano, P. R. Structure and catalytic mechanism of horseradish peroxidase: region specific meso alkylation of the prosthetic heme group by alkylhydrazines. *J. Biol. Chem.* **262**, 14954–14960 (1987).
18. Arnao, M. B., Acosta, M., Del Rio, J. A. & Garcia-Canovas, F. Inactivation of peroxidase by hydrogen peroxide and its protection by a reductant agent. *Biochim. Biophys. Acta.* **1038**, 85–89 (1990).
19. Choi, Y. J., Chae, H. J. & Kim, E. Y. J. Steady-state oxidation model by horseradish peroxidase for the estimation of the noninactivation zone in the enzymatic removal of pentachlorophenol. *Biosci. Bioengin.* **88**, 368–373 (1999).
20. Huang, Q. *et al.* Inactivation of horseradish peroxidase by phenoxyl radical attack. *J. Am. Chem. Soc.* **127**, 1431–1437 (2005).
21. Buchanan, I. D. & Nicell, J. A. Kinetics of peroxidase interactions in the presence of a protective additive. *J. Chem. Technol. Biotechnol.* **72**, 23–32 (1998).

22. Caza, N., Bewtra, J. K., Biswas, N. & Taylor, K. E. Removal of phenolic compounds from synthetic wastewater using soybean peroxidase. *Water Res.* **33**, 3012–3018 (1999).

23. Wu, Y., Taylor, K. E., Biswas, N. & Bewtra, J. K. Comparison of additives in the removal of phenolic compounds by peroxidase catalyzed polymerization. *Water Res.* **31**, 2699–2704 (1997).

24. Nicell, J. A. Kinetics of horseradish peroxidase-catalyzed polymerization and precipitation of aqueous 4-cholorophenol. *J. Chem. Technol. Biotechnol.* **60**, 203–215 (1994).

25. Colosi, L. M., Huang, Q. & Weber, W. J. Jr. Quantitative structure activity relationship based quantification of the impacts of enzyme-substrate binding on rates of peroxidase-mediated reactions of estrogenic phenolic chemicals. *J. Am. Chem. Soc.* **128**, 4041–4047 (2006).

26. Poulos, T. L. & Kraut, J. The stereochemistry of peroxidase catalysis. *J. Biol. Chem.* **255**, 8199–8205 (1980).

27. Rodríguez-López, J. N. *et al.* Mechanism of reaction of hydrogen peroxide with horseradish peroxidase: Identification of intermediates in the catalytic cycle. *J. Am. Chem. Soc.* **123**, 11838–11847 (2001).

28. Dawson, J. H. Probing structure-function relations in heme containing oxygenases and peroxidases. *Science* **240**, 433–439 (1988).

29. Huang, L., Colas, C. & Ortiz de Montellano, P. R. Oxidation of carboxylic acids by horseradish peroxidase results in prosthetic heme modification and inactivation. *J. Am. Chem. Soc.* **126**, 12865–12873 (2004).

30. Pipirou, Z. *et al.* The reactivity of heme in biological systems: autocatalytic formation of both tyrosine-heme and tryptophan-heme covalent links in a single protein architecture. *Biochemistry* **46**, 13269–13278 (2007).

31. Huang, L., Wojciechowski, G. & Ortiz de Montellano, P. R. Prosthetic heme modification during halide ion oxidation. Demonstration of chloride oxidation by horseradish peroxidase. *J. Am. Chem. Soc.* **127**, 5345–5353 (2005).

32. Wojciechowski, G., Huang, L. & Ortiz de Montellano, P. R. Autocatalytic modification of the prosthetic heme of horseradish but not lactoperoxidase by thiocyanate oxidation products. A role for heme-protein covalent cross-linking. *J. Am. Chem. Soc.* **127**, 15871–15879 (2005).

33. Lad, L. *et al.* Crystal structure of human heme oxygenase-1 in a complex with biliverdin. *Biochemistry* **43**, 3793–3801 (2004).

34. Ortiz de Montellano, P. R. Control of the catalytic activity of prosthetic heme by the structure of hemoprotein. *Acc. Chem. Res.* **20**, 289–294 (1987).

35. Wojciechowski, G. & Ortiz de Montellano, P. R. Radical energies and the regiochemistry of addition to heme groups. Methylperoxy and nitrite radical additions to the heme of horseradish peroxidase. *J. Am. Chem. Soc.* **129**, 1663–1672 (2007).

36. Denisov, E. & Denisova, T. Dissociation energies of O-H bonds of phenols and hydroperoxides. In *Application of thermodynamics to biological and materials science* (ed Mizutani, T.). ISBN: 978-953-307-980-6, In Tech, p406–440 (2011). (Available from: http://cdn.intechopen.com/pdfs/13122/InTech-Dissociation_ energies_of_o_h_bonds_of_phenols_and_hydroperoxides.pdf. Date of access, August 24 2013).

37. Colosi, L. M., Huang, Q. & Weber, W. J. Jr. Validation of a two-parameter quantitative structure activity relationship as a legitimate tool for rational redesign of horseradish peroxidase. *Biotechnol. Bioeng.* **98**, 295–299 (2007).

38. Strutt, J., Wilson, S., Shorney-Darby, H., Shaw, A. & Byers, A. Assessing the carbon footprint of water production. *J. Am. Water Works Assoc.* **100**, 80–91 (2008).

39. Lu, J., Huang, Q. & Mao, L. Removal of acetaminophen using enzyme-mediated oxidative coupling processes: Reaction rates and pathways. *Environ. Sci. Technol.* **43**, 7062–7067 (2009).

40. Mao, L. *et al.* Ligninase-mediated removal of natural and synthetic estrogens from water: II. Reactions of 17β-estradiol. *Environ. Sci. Technol.* **44**, 2599–2604 (2010).

41. Davies, E. M. Protein assays: A review of common techniques. *Amer. Biotech. Lab.* July, 28–37 (1988).

42. Putter, J. & Becker, R. Peroxidases. In *Methods of Enzymatic Analysis* (ed Bergmeyer, H. U., Bergmeyer, J. & Grassl, M.) 286–293 (Verlag Chemie, Deerfield Beach, 1983).

Acknowledgements

Author contributions

L.M. carried out figures preparation, main experiments, and data interpretations and wrote the manuscript. S.L. performed research on LC-MS. L.M. and Q.H. designed research. J.L. contributed to data interpretations. All authors contributed to scientific discussions.

Additional information

Competing financial interests: The authors declare no competing financial interests.

How to cite this article: Mao, L., Luo, S., Huang, Q. & Lu, J. Horseradish Peroxidase Inactivation: Heme Destruction and Influence of Polyethylene Glycol. *Sci. Rep.* **3**, 3126; DOI:10.1038/srep03126 (2013).